

Radiation Dose Optimization for Critical Organs in Interventional Radiology

Yasaman Khodadadegan, Muhong Zhang and William Pavlicek
School of Computing, Informatics, and Decision Systems Engineering
yasaman.khodadadegan@asu.edu and muhong.zhang@asu.edu

OBJECTIVE

To provide a setting for the equipment in terms of geometry and energy which minimizes the absorbed dose in a critical organ while maintaining image quality.

INTRODUCTION

- Imaging modality: Fluoroscopically Guided Interventional (FGI),
- The X-ray passes through the patient \Rightarrow attenuated while interacting with the different internal structures of the body \Rightarrow a shadow of the structures constructs the digital image.
- Two major types of risks: deterministic (skin injuries) and stochastic effects (cancer induction),
- Any amount of the absorbed radiation in the body \propto a risk of cancer induction

FGI MODALITY

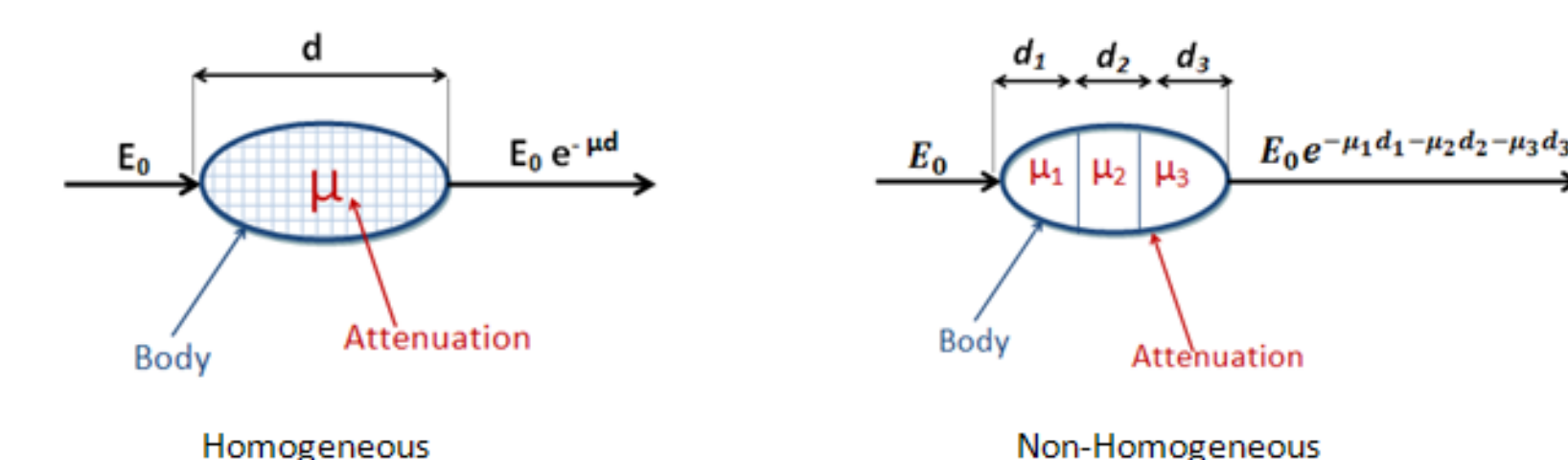


Siemens.medical.com

ASSUMPTIONS

- Patient and image are discretized in pseudo voxels with equal size.
- A set of CT images are used for the estimate of attenuation coefficient for each voxel at a given kV.
- Table attenuation is not considered in the computations.
- The distance traversed in each pseudo voxel by the pencil beam is assumed to be equal.
- Energy of the beam is uniformly distributed and equal for each pencil beam.
- Each pencil beam is emitted from the X-ray source to the center of a pseudo pixel in the image.

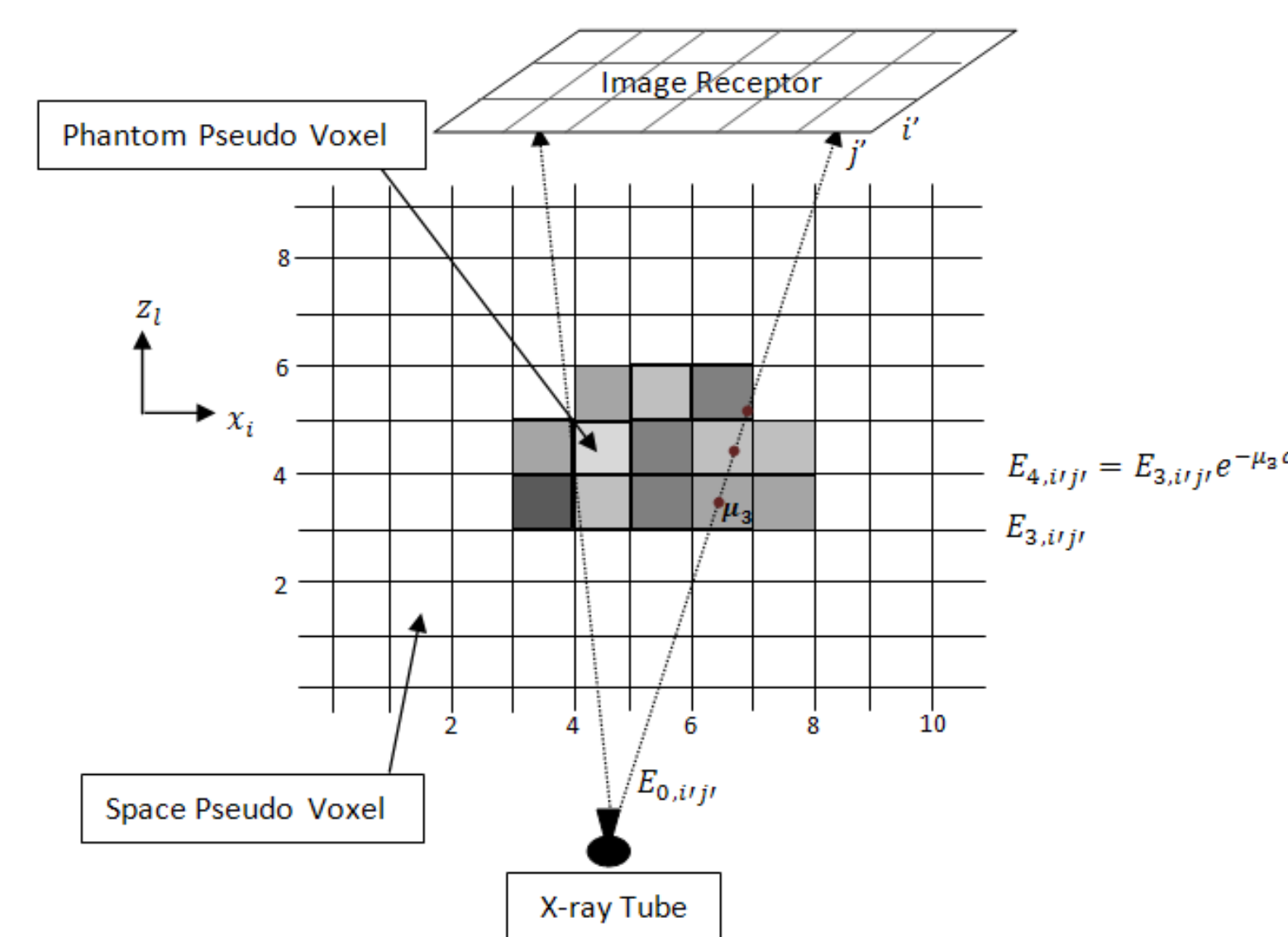
X-RAY ATTENUATION



MOTIVATION

- More than 700,000 fluoroscopy examinations are performed everyday in US [?].
- A linear, no-threshold (LNT) model illustrates the dose and cancer risk relationship (Nuclear Regulatory Commission (NRC)).
- A study on women who received chest X-ray: young women who receive repeated X-rays with breast tissue included in the beam interception region with body, have about 9 times higher potential risk of breast cancer for the ages ≤ 40 in compare with ages > 40 [?].

NOTATIONS



E_0 : Initial energy of each beam at source
 $E_{l_p, i'j'}$: energy of beamlet $i'j'$ at level l_p
 $\gamma_{i'j'}$: indicator of beamlet existence in the field of radiation
 x_i, y_j, z_l : table increments in each direction
 $\psi_{(i_p, j_p, l_p), i'j'}$: indicator of voxel i_p, j_p, l_p of body interception with beamlet $i'j'$

MATHEMATICAL MODEL

$$\text{Min } \sum_{V_{(i_p, j_p, l_p)} \in C_o} \text{dose}_{V_{(i_p, j_p, l_p)}} = \sum_{(i_p, j_p, l_p): V_{(i_p, j_p, l_p)} \in C_o} \sum_{i'j'=1}^{n^2} \frac{\Gamma_{(i_p, j_p, l_p), i'j'} (1 - e^{-\mu_{(i_p, j_p, l_p)} d})}{m_{V_{(i_p, j_p, l_p)}}}$$

Subject to

- Constraints to identify which pseudo pixels of the detector are in the field.

$$\gamma_{i'j'} \leq \eta_{i'} \quad (1)$$

$$\gamma_{i'j'} \leq \delta_{j'} \quad (2)$$

$$\gamma_{i'j'} \geq \eta_{i'} + \delta_{j'} - 1 \quad (3)$$

$$\delta_{j'} \geq \delta_p + \delta_t - 1 \quad (4)$$

$$p \leq j' \leq t, \quad p = 1, \dots, n-2, \quad t = p+2, \dots, n \quad (5)$$

$$\eta_{i'} \geq \eta_k + \eta_h - 1 \quad (5)$$

$$k \leq i' \leq h, \quad k = 1, \dots, n-2, \quad h = k+2, \dots, n,$$

- Constraint to determine the patient voxels position and interception with beams

$$\beta_{(i_p, j_p, l_p), (\hat{i}, \hat{j}, \hat{l}), i'j'} \leq \psi_{(i_p, j_p, l_p), i'j'} \quad (6)$$

$$\forall (i_p, j_p, l_p) \in VP, (\hat{i}, \hat{j}, \hat{l}) \in S_{i'j'}$$

$$\text{s.t. } \hat{i} = i + i_p, \hat{j} = j + j_p, \hat{l} = l + l_p, \quad i', j' = 1, \dots, n$$

$$\psi_{(i_p, j_p, l_p), i'j'} \leq \gamma_{i'j'} \quad (7)$$

$$\exists \beta_{(i_p, j_p, l_p), (\hat{i}, \hat{j}, \hat{l}), i'j'} \leq x_i + y_j + z_l \quad (8)$$

$$\beta_{(i_p, j_p, l_p), (\hat{i}, \hat{j}, \hat{l}), i'j'} \leq \xi_{(i_p, j_p, l_p), (\hat{i}, \hat{j}, \hat{l}), i'j'} \quad (9)$$

$$\psi_{(i_p, j_p, l_p), i'j'} \leq \sum_{(\hat{i}, \hat{j}, \hat{l}) \in S_{i'j'}} \beta_{(i_p, j_p, l_p), (\hat{i}, \hat{j}, \hat{l}), i'j'} \quad (10)$$

$$\beta_{(i_p, j_p, l_p), (\hat{i}, \hat{j}, \hat{l}), i'j'} - (x_i + y_j + z_l + \gamma_{i'j'}) \geq \xi_{(i_p, j_p, l_p), (\hat{i}, \hat{j}, \hat{l}), i'j'} - 4 \quad (11)$$

- Constraint to linearize the objective function

$$\Gamma_{(i_p, j_p, l_p), i'j'} \geq E_{l_p, i'j'} - M(1 - \psi_{(i_p, j_p, l_p), i'j'}) \quad (12)$$

- Constraints to connect different levels of energy of a beam

$$E_{l_p-1, i'j'} \leq E_{l_p, i'j'} + M \sum_{i_p, j_p \in VP} \psi_{i_p, j_p, l_p-1, i'j'} \quad (13)$$

$$E_{l_p, i'j'} \geq E_{l_p-1, i'j'} e^{-\mu_{i_p, j_p, l_p-1} d} - M(1 - \psi_{i_p, j_p, l_p-1, i'j'}) \quad (14)$$

MATHEMATICAL MODEL

$$E_{l_p, i'j'} \leq E_{l_p-1, i'j'} e^{-\mu_{(i_p, j_p, l_p-1)} d} + M(1 - \psi_{(i_p, j_p, l_p-1), i'j'}) \quad (15)$$

$$\sum_{i_p \in VP} \sum_{j_p \in VP} \psi_{(i_p, j_p, l_p), i'j'} \leq 1 \quad (16)$$

$$\sum_{i'=1}^n \sum_{j'=1}^n \psi_{(i_p, j_p, l_p), i'j'} \geq 1, \quad \forall (i_p, j_p, l_p) \in ROI \quad (17)$$

- Image quality constraint

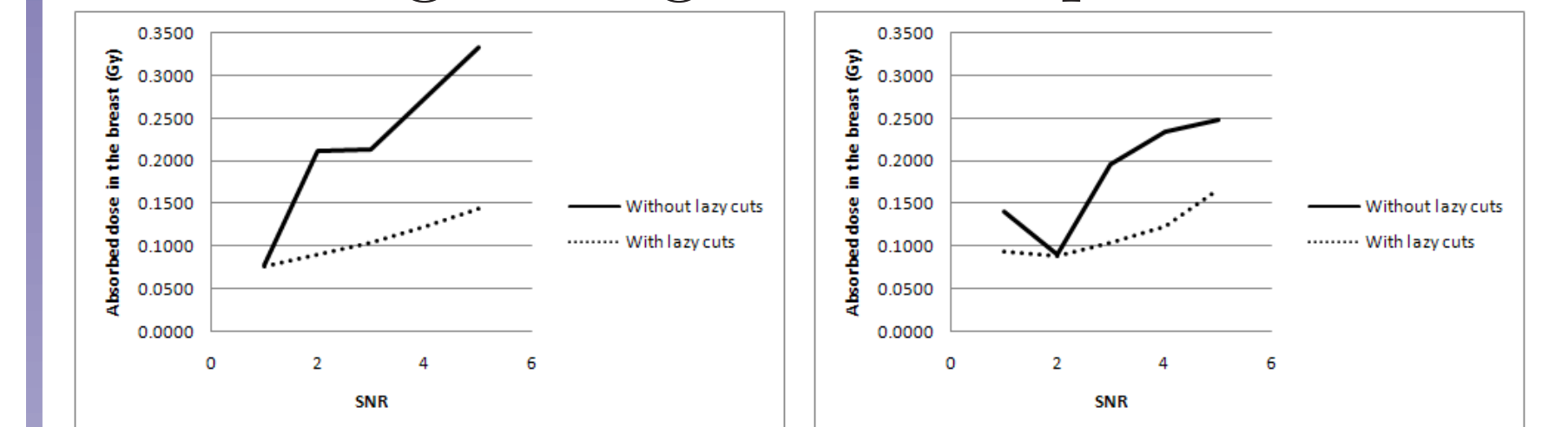
$$K_1'' \sum_{i'=1}^n \sum_{j'=1}^n \alpha_{i'j'} \leq \sum_{i'=1}^n \sum_{j'=1}^n \tau_{i'j'} \quad (18)$$

$$\sum_{i'=1}^n \sum_{j'=1}^n \tau_{i'j'} \leq K_2'' \sum_{i'=1}^n \sum_{j'=1}^n \alpha_{i'j'} \quad (19)$$

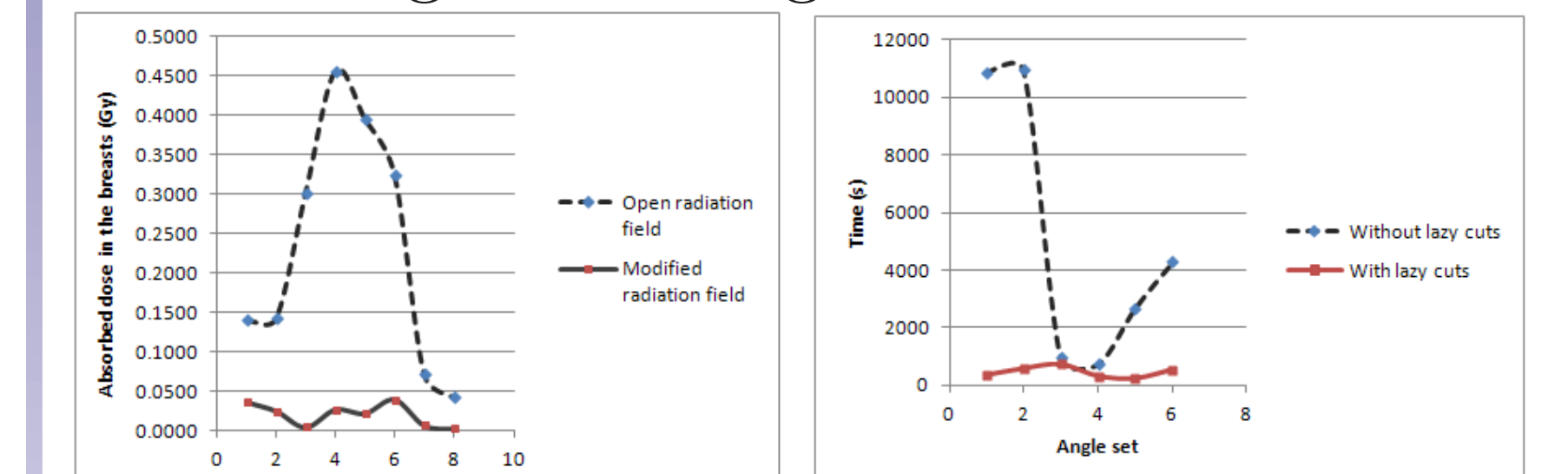
RESULTS

Using polyhedral analysis, we added strong valid inequalities to the lazy cut pool. We solved a number of test problems for cardiovascular exams where patient breasts are critical organs and patient heart is organ of interest. Then we added some search algorithms to the preprocessing step of CPLEX12.

- Adding Strong Valid Inequalities



- Adding Search Algorithm



Angle	Absorbed dose in the breasts (Gy)	Radiation field size	Absorbed dose in the breasts (Gy)	Radiation field size	Number of pseudo pixel increments	Dose reduction percentage in the breast	
Primary	Secondary	Complete field size	(cm ²)	Smaller field size	(cm ²)	x y z	
0	0	0.1407	37.45	0.0363	3.51	1 0 34	74.20%
-10	0	0.1428	38.92	0.0251	18.73	1 -6 22	82.42%
15	0	0.3021	38.92	0.0045	14.04	1 9 12	98.51%
20	0	0.4551	37.45	0.0271	23.41	2 9 -1	94.05%
30	0	0.3948	37.45	0.0220	28.09	3 15 1	94.43%
-20	0	0.3239	37.45	0.0397	16.39	1 -11 6	87.74%
15	10	0.0718	37.45	0.0069	4.68	-3 12 19	90.39%
-20	20	0.0426	37.45	0.0024	11.70	-6 -9 -3	94.37%